analytical chemistry

Article

pubs.acs.org/ac

Highly Sensitive Capacitive Gas Sensing at Ionic Liquid–Electrode Interfaces

Zhe Wang,[†] Min Guo,[†] Xiaoyi Mu,[‡] Soumyo Sen,[§] Thomas Insley,[§] Andrew J. Mason,[‡] Petr Král,[§,∥,⊥] and Xiangqun Zeng*[,†]

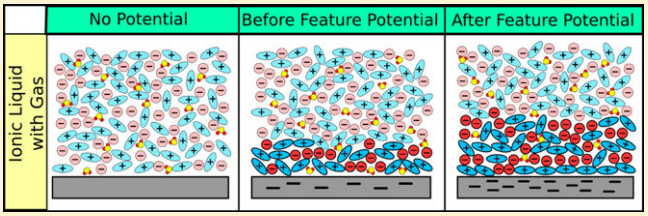
[†]Department of Chemistry, Oakland University, Rochester, Michigan 48309, United States

[‡]Department of Electrical & Computer Engineering, Michigan State University, East Lansing, Michigan 48824, United States

[§]Departments of Chemistry, [∥]Physics, and [⊥]Biopharmaceutical Sciences, University of Illinois at Chicago, Chicago, Illinois 60607, United States

Supporting Information

ABSTRACT: We have developed an ultrasensitive gas-detection method based on the measurement of a differential capacitance of electrified ionic liquid (IL) electrode interfaces in the presence and absence of adsorbed gas molecules. The observed change of differential capacitance has a local maximum at a certain potential that is unique for each type of gas, and its amplitude is related to the concentration of the gas molecules. We establish and validate this gas-sensing method by characterizing SO_2 detection at ppb levels with less than 1.8% signal from other interfering species (i.e., CO_2, O_2, NO_2, NO, SO_2, H_2O, H_2, and cyclohexane, tested at the same concentration as SO_2). This study opens a new avenue of utilizing tunable electrified IL–electrode interfaces for selective sensing of molecules with a kinetic size resolution of 0.1 Å.



Ionic liquids (ILs) are a class of compounds containing bulky organic ions that melt close to room temperature.[1,2] In recent decades, their unique properties both as solvents and electrolytes have spurred significant research activities. One of the most active areas of research is the examination of IL properties at charged electrode interfaces. Numerous reports have shown that IL–electrode interfaces behave fundamentally differently from bulk ILs and cannot be described by the Gouy–Chapman–Sterns double layer model, used in aqueous electrolytes.[3−6] A helium atom-scattering technique was used to characterize surface structure and phase transitions of $[C_2C1Im][NTf_2]$ ionic liquid on Au(111). The formation of successive ordered layers of ion pairs during adsorption of $[C_2C1Im][NTf_2]$ on Au (111) was observed.[7] Atomic force microscopy (AFM) studies performed at open-circuit potentials of ±1–2 V have also revealed that relatively large forces (~5–20 nN) are required to rupture the innermost IL layer by an AFM tip and make contact with the electrode surface.[8,9] Molecular dynamics simulations revealed that this IL layer above the charged electrodes has a highly compact and viscous structure.[10,11] Bulky (polar) ions self-assemble at IL–electrode interfaces according to local Coulombic, van der Waals (vdW), and steric forces.[12−15] The structure of IL interface with adsorbed gas molecules can be controlled by the electrode potential.[16−20] The inner layer of IL–metal interface was reported to have 0.2–2 nm thickness under an applied dc potential,[21] which is comparable with kinetic diameters (KDs) of most gas molecules at room temperature. Molecular dynamics (MD) simulations of 10 different pure and CO_2-saturated ionic liquids have shown a strong correlation between the ratio of unoccupied space in pure ILs and their ability to absorb CO_2.[22] Furthermore, MD simulations of a water distribution at $[Bmim][PF_6]$–electrode interface show that the preferential positions of water molecules in double layers are determined by the balance of several factors: the tendency to follow the positions of the maximal absolute value of the electrical field, the association with their ionic surroundings, and the propensity to settle at positions where more free space is available. However, electrified IL–electrode interfaces with adsorbed gas molecules have not been experimentally studied.[23]

Our early work has demonstrated that the high viscosity of ILs that is usually considered a limitation to practical electrochemical applications, due to slow rate of mass transport, is an advantage in capacitance measurement for methane, allowing quantitative determination of methane concentration based on the change of the differential capacitances at the IL–electrode interface.[24] This study led us to hypothesize that the ability of an IL–electrode interface for preferentially incorporating specific gas molecules could be tuned by the applied dc potential. This would allow for a sensitive and selective adsorption and detection of small gas molecules, depending on their dipole moments and their KDs.[25,26] In this work, we intend to validate this hypothesis and to answer several fundamental questions related to gas adsorption at the electrified IL–electrode interface: (1) How do gas species

Received: December 10, 2015
Accepted: December 25, 2015
Published: December 25, 2015

ACS Publications © 2015 American Chemical Society

DOI: 10.1021/acs.analchem.5b04677
Anal. Chem. 2016, 88, 1959–1964

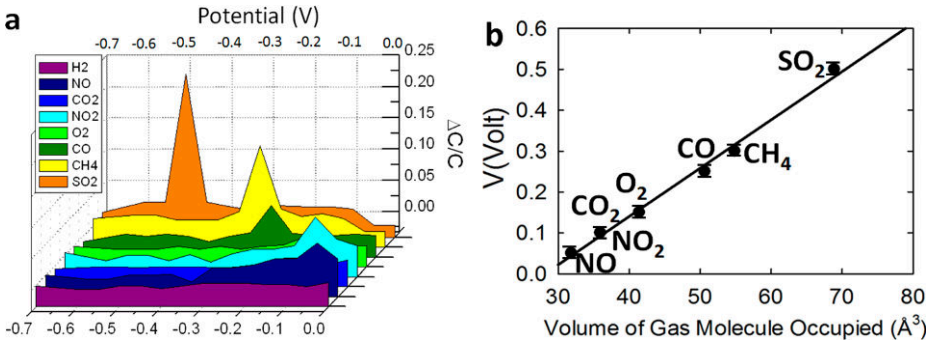


Figure 1. Feature potentials of gases with different kinetic sizes at the IL/Au interface. (a) Capacitance−potential curves when the IL−electrode interface was exposed to eight gases, respectively. Potential scanned from −0.7 to 0 V. No faradaic processes in this potential window for the gases tested in this work. (b) Plot of feature potential (V) of tested gases vs their molecular volume (directly related to KD^3).

(i.e., the analyte) interact with the ions at varying applied potentials at the IL−electrode interface? (2) How does the differential capacitance change upon the adsorption of the gas analyte at a certain potential? (3) What is the relationship of the differential capacitance change with electric potential and the properties of the gas analyte (i.e., the dipole moments and sizes of the gas analytes). We characterize in electrochemical impedance experiments the IL/Au double layer capacitance in the presence of eight common gas molecules (i.e., SO_2, CO_2, O_2, NO_2, NO, SO_2, H_2O, and H_2) at different dc bias potentials. We select IL $[C_4mpy][NTf_2]$ where both cations and anions are large and have weak electrostatic cation−anion interaction densities. This may lead to the presence of a large number of unoccupied spaces in the IL. We characterized the IL/electrified electrode interface at various potentials. The change of differential capacitance signals at IL/Au interface in the presence of each of the eight gas molecules was correlated with their dipole moments and kinetic diameters. Quantitative detection of SO_2 at ppb level in the presence of common interfering gas species was demonstrated.

EXPERIMENTAL SECTION

A novel, interdigitated electrode was fabricated on a gas-permeable membrane and utilized in electrochemical impedance experiments (Supporting Information and Figure S1). The microfabricated electrode was equipped with a back-flow gas-sampling system, allowing the presence of gas molecules at the IL−electrode interface.[24,27] (Figure S1). As shown in the Bode plots of the electrochemical impedance spectrum (EIS) (Figure S3) at frequency range 0.1−3 Hz, at very low frequencies the phase angle is close to −90°, confirming that the IL−Au electrode interface behaves like a pure capacitor, where the real part (C_{re}) defines the capacitance of the electrochemical system.[28] The capacitance change is attributed to the interface rather than to the bulk ionic liquid (Supporting Information and Figure S2). Gas molecules present at the IL/Au interface can be selectively sensed by measuring the change of the electrode capacitance at low frequency. The mass flow controllers were used to adjust the ratio of the analyte gas and nitrogen flow rates. The total gas flow was set at 200 sccm (standard cubic centimeters per minute), and it was maintained as a constant at atmospheric pressure. EIS testing was carried out with a VersasStat MC potentiostat (Princeton Applied Research, Oak Ridge, TN, U.S.A). A dc bias plus a sinusoidal ac signal with 10 mV peak-to-peak amplitude was applied for sensing SO_2.

RESULTS AND DISCUSSION

We first studied the potential-dependent capacitance change when each of the eight common gases with different molecular sizes (i.e., H_2, CO_2, NO, O_2, NO_2, CO, CH_4, and SO_2) was separately introduced into the IL−Au electrode interface at an applied dc potential between 0 and −0.7 V (vs Pt reference electrode). The KD values of target gases are listed in Table S1. We do not expect that there is a substantial reactive charge transfer between the chosen molecules and the electrode in the potential range studied. However, we assume that the IL−electrode interface has different amounts and sizes of unoccupied spaces at different applied dc potentials, and the potential can tune the crystalline ordering of the ILs, generating optimal structure and properties of the unoccupied spaces and enabling selective adsorption of a specific size of gas molecule.

Figure 1a shows that the capacitance change for each of the gases studied has a large maximum at a specific potential, called here a "feature potential". Varying the potential in the smallest interval (±0.03 V) led to the differential capacitance signal being dropped to 10% of maximum at feature potential ±0.03 V and the differential capacitance signal being dropped to 1% of the maximum when the potential is at feature potential ±0.05 V. For example, the feature potential for methane (KD = 0.38 nm) is −0.3 V, and for SO_2 (KD = 0.41 nm) it is −0.5 V. Interestingly, NO_2 and CO_2, both with KDs of 0.33 nm, have almost the same feature potential. These results suggest that the gas analyte within the IL−electrode interface undergoes a large rearrangement around the feature potentials,[29] depending on the analyte KD values and dipole moments, as evidenced in Figure 2b.[30,31] While the position change of smaller gas molecules takes part at lower feature potentials, larger molecules rearrange at significantly higher potentials.

Our experimental results also show that the differential capacitance change mainly comes from the IL−electrode interface. When gas molecules are dissolved in the bulk IL, no change of the differential capacitance was observed. The relative permittivity of the gas molecules (i.e., CO_2, O_2, NO_2, NO, SO_2, H_2, and cyclohexane) we studied in this work is greater than one but much smaller than that of the IL. Gas adsorption may increase the relative permittivity and thus the differential capacitance; this increase is negligible, and the relative static permittivity in the presence of different gas molecules can be treated as a constant. Thus, selective sensing of gas molecules with certain kinetic diameters (KDs) at the IL−electrode interface is more of a result of the change of the effective thickness of the interface layer. The adsorption of gas

DOI: 10.1021/acs.analchem.5b04677
Anal. Chem. 2016, 88, 1959−1964

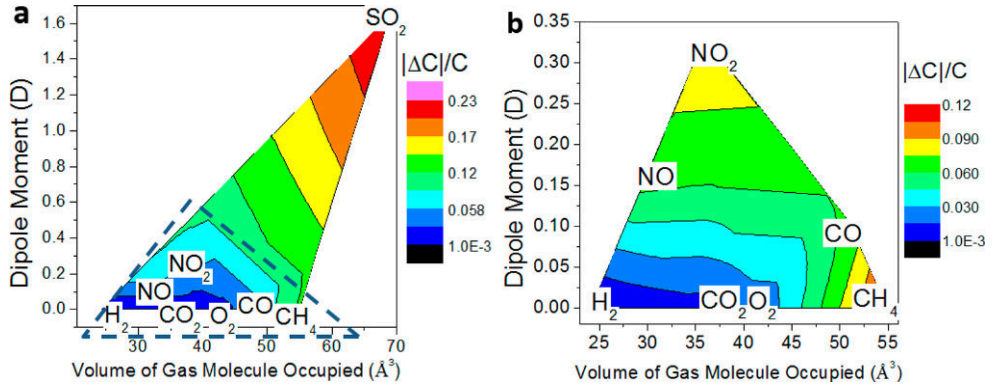


Figure 2. Measured capacitance response of various gases plotted as a function of their molecular dipole moments (*y*-axis) and molecular volumes (*x*-axis). (a) The capacitance response generally increases with dipole moment and molecule volume. (b) Enlarged triangle area in (a).

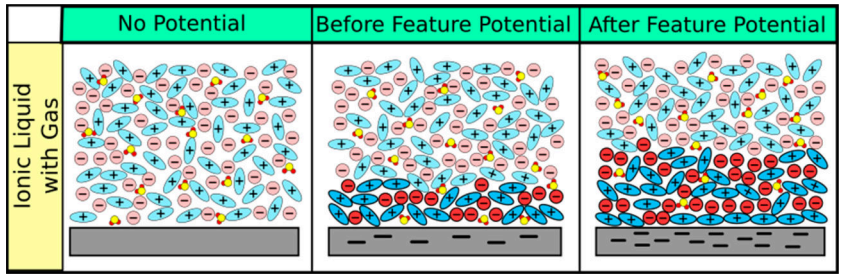


Figure 3. Schematics of ionic liquid/Au interface for gas adsorption at various bias potentials.

molecules at low potentials and open-circuit potential does not affect the overall organization of the ions at the IL interface, likely due to the large size and numbers of unoccupied spaces available in the IL.

Figure 2 shows the $\Delta C/C$ distribution as a function (color contours) of dipole moments and sizes (KD) of the gas molecules. $\Delta C/C$ increased with the increase of the dipole moments. NO_2 and CO_2 have similar KDs (0.33 nm), but NO_2 is more polar, which gives a bigger signal. The $\Delta C/C$ signals for nonpolar molecules, H_2, CO_2, O_2, and CH_4, increased slightly with their molecule sizes. In the presence of an electric field, nonpolar molecules such as CH_4 can also have an induced dipole moment. For CH_4, there is an additional Au−H formation at the electrode between −0.5 and 0.1 V;[32] this might be related to the fact that CH_4 gives the second largest signal among the tested gases. SO_2, with the largest size and biggest dipole moment, promoted the highest change of the double layer thickness and the dielectric constant of the IL interface, and it shows the largest change of the signal.

As summarized in Figure 3, we rationalize that, at the feature potential, the adsorbed gas molecule is being expelled from the IL interface by the induced-ion rearrangement, reducing the number and size of unoccupied spaces at IL−electrode interface to be smaller than values tolerable by the gas molecules. This would lead to a measurable capacitance change. The selectivity of the sensing should come from the combined effects of the shape and size of the unoccupied space, which depends on the cation and anion of the specific ionic liquid, and the association of gas molecules with their ionic surroundings, which depends on the properties of the gas molecules, particularly its size and polarity, and the applied dc potential. The ionic liquid structure at an electrified interface determines the amount and size of the unoccupied space, and the applied electric field can fine-tune the interface structure and properties. The unique interactions of the gas molecules with their ionic environmental subsequently determines the sensitivity and selectivity of gas sensing. Thus, gas molecules with different KDs and dipole moments, in principle, can be detected at different electrode potentials, which is reflected in the capacitance change. The largest capacitance change at the IL−electrode interface, which occurs at the feature potential, is specific to certain gas molecules and, in principle, can be used to identify the gas species based on its KD. Such a molecular "spectrum" primarily depends on its kinetic size, similar to a mass spectrum, as discussed later. However, the relative capacitance change ($\Delta C/C$) is governed by other factors as well. At the electrified IL−electrode interface, counterions condense at the electrified metal surface to form compact ion-image dipoles.[33] At the interface, ions are polarizable both through electrons reorganization and their orientation when being polar (permanent dipole moments follow the local field). The possibility of insertion of a gas molecule in this IL−electrode assembly is determined by the density of these dipoles (potential), the size and polarity of the gas molecules, and the structure of the IL interface double layers.

We further validate our rationalization by characterizing SO_2 detection. Figure 4 summarizes the analytical characterization of the IL−electrode interface at SO_2 feature potential for the detection and quantification of SO_2 through the capacitive measurements. In Figure 4a, the real capacitance (C_{re}) at SO_2 feature potential (−0.5 V) decreased from 43.3 to 13.3 μF in the presence of 25 ppm of SO_2. The relationship of C_{re} versus SO_2 concentration follows a nonlinear relationship, which can be quantified using a Langmuir adsorption model (Supporting Information). Defining C_{dl0} as the double layer capacitance when the surface coverage θ is zero and C_{dl1} as the double layer capacitance when θ is equal to 1, we obtain

DOI: 10.1021/acs.analchem.5b04677
Anal. Chem. 2016, 88, 1959−1964

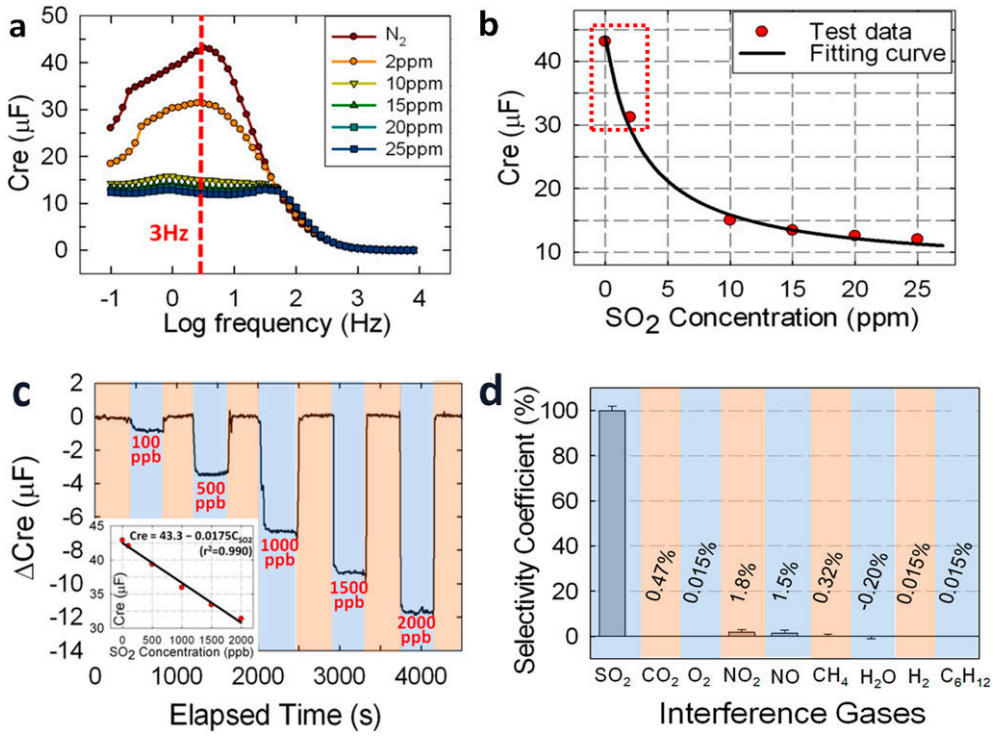


Figure 4. SO_2 detection at its feature potential of kinetic size spectra. (a) Real part of complex capacitance plot in frequency range of 100 mHz to 10 kHz with different sulfur dioxide concentrations; (b) real part of complex capacitance at 3 Hz vs SO_2 concentration curve. At low concentration of SO_2, the responses are close to linear. (c) ΔC_{re} at 3 Hz measured over five cycles of alternate exposure to 0−2 ppm of SO_2 in a dry nitrogen condition at an applied potential of −0.5 V. Inset is the calibration curve with the sensitivity of 0.0175 uF/ppb at dynamic range of 0−2000 ppb. (d) Selectivity coefficients of SO_2 vs primary interfering gaseous species (0.015−1.8%) measured at −0.5 V at 3 Hz. The gas flow rate is maintained at 200 sccm.

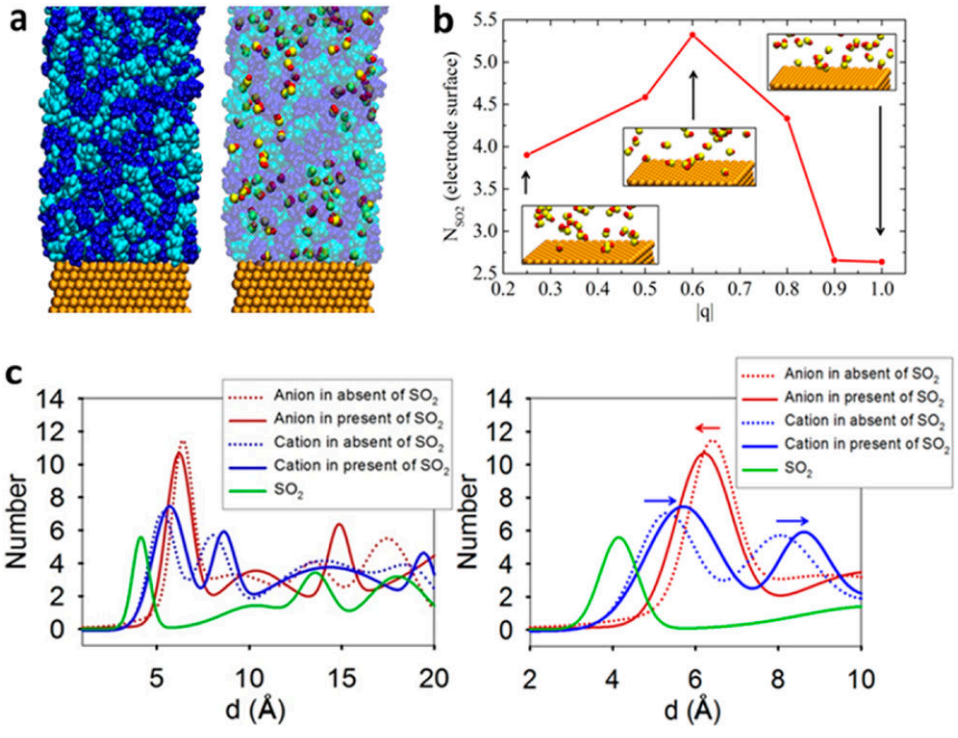


Figure 5. Atomistic MD simulations of $[C_4mpy][NTf_2]$ ionic liquid on a charged gold surface (two atomic layers are charged) and a gas-selection scheme. (a) Left in the absence and right in the presence of SO_2 molecules. The cations and anions are visualized in dark and light blue, respectively, gold atoms are in orange, and sulfur and oxygen of SO_2 gas molecules are in yellow and red, respectively. (b) Number of SO_2 molecules within the first peak, separated 4 Å away from the surface, obtained at different surface chargings. Figure S6 includes detailed data. (c) Distribution of ions of ionic liquid and SO_2 molecules with the distance from the gold surface at $-0.6e$ in the absence (dash curve) and in the presence (solid curve) of SO_2 gas molecules. Left is 0−2.0 nm and right is inner layer (0.2−1.0 nm) of the distance from the gold surface at $-0.6e$. Nonfitted data are shown in Supporting Information note 4 and Figure S5.

DOI: 10.1021/acs.analchem.5b04677
Anal. Chem. 2016, 88, 1959−1964

$$C_{dl} = C_{dl0} + (C_{dl1} - C_{dl0})\frac{KC_{SO_2}}{1 + KC_{SO_2}} \quad (1)$$

Here, θ is the surface coverage of SO_2 at the Au electrode, C_{SO_2} is the concentration of SO_2, and $K = k_H \times K_1$ (K_1 is the ratio of the forward and backward rate constants in the adsorption equivalent equation and k_H is defined as the Henry constant of SO_2 in $[C_4mpy][NTf_2]$).[24] Using eq 1 to fit data at 3 Hz in Figure 4a, the fitting curve is plotted as the black line in Figure 4b. The relationship between C_{re} and C_{SO_2} is

$$C_{re} = 43.34\ \mu F - 30.00\ \mu F\frac{C_{SO_2}}{C_{SO_2} + 3.06\ ppm} \quad (R^2 = 0.9990) \quad (2)$$

where surface area is 8.4×10^{-6} m^2. The normalized eq 2 is $C_{re}(F/m) = 5.16F/m - 3.57F/m\frac{C_{SO_2}}{C_{SO_2} + 3.06\ ppm}$

It shows that the sensitivity is especially high at low SO_2 concentrations. SO_2 has the largest dipole moment of 1.62 D among the tested gas molecules. The electrode adsorption of SO_2 leads to a significant change of the interface capacitance, especially at low concentration. This allows for the detection of trace amounts of SO_2 at ppb levels. At the low concentration range (the red dotted line range of Figure 4b), the relationship of ΔC_{re} vs C_{so_2} is close to linear. A real-time detection of low concentration of SO_2 was also measured by the single frequency method, as shown in Figure 4c. Its response time is <10 s, and the detection limit is <30 ppb. It confirms the flexibility and stability of the IL−electrode interface, allowing real-time and long-term measurements (Figure S4).

Figure 4d shows that the selectivity coefficients of SO_2 relative to CO_2, O_2, NO_2, NO, SO_2, H_2O, H_2, and cyclohexane are <1.8% (Supporting Information). This means that the SO_2 detection at the feature potential (−0.5 V) shows excellent selectivity. All interference gases decrease the IL−Au interface capacitance except H_2O, which was found to increase the double layer capacitance, thus indicating a negative signal in Figure 4d. This trend was observed in our previous work about water effect.[24] The adsorbed water would form a new double layer of water/Au, and the permittivity of water (81 F/m) is much higher than that of $[C_4mpy][NTf_2]$ (11.7 F/m).[34] A similar phenomenon was found in a single-walled carbon nanotube (SWNT) capacitor sensor as well.[35]

To better understand the fundamentals of the observed sensing phenomena, we carried out simple molecular dynamics (MD) simulations of gas molecules at an electrified IL interface. To interpret these simulation results, we should first recognize that the behaviors of ILs at the metallic interface are highly complex in reality, due to ion-induced dynamical polarization of the surface (image charges). This complex behavior of an electrified IL interface was modeled by Monte Carlo simulations,[36] revealing that the capacitance of the interface can be very large at small biases V, where the coupling of ions to each other and to their surface images is larger than the thermal energy ($kT < e^2/a$)

$$C(V) = \frac{8}{3}\left(\frac{1}{10\alpha}\right)^{2/3}\left(\frac{e}{aV}\right)^{1/3}\frac{1}{a} \approx 1.3\left(\frac{e}{aV}\right)^{1/3} C_H = \varepsilon_0\varepsilon_{IL}\frac{A}{d} \quad (3)$$

Here, α is a numerical coefficient that describes the structure of the lattice of excess ion, a is the ion diameter, and C_H is the Helmholtz capacitance. C_H describes a situation where counterions are collapsed on the nonpolarized surface, in contrast to the high-temperature case, where they are within a Debye length from it. Equation 3 implies that the capacitance can be significantly larger than C_H when V is small. Thus, the effective thickness of the double layer, d (right side), can be smaller than the ion radius, due to the ability of IL ions to form image charges at the metal surface.[36] Here, ε_0 is the vacuum permittivity (8.854×10^{-12} F m^{-1}), ε_{IL} is the relative static permittivity of IL, and A is the cumulated layer area. Equation 3 gives the relationship $V^{1/3} \approx d$, between the applied potential, V, and the effective double layer thickness, d. The effective double layer thickness d should correlate well to the unoccupied space, which is also correlated to the effective size D of the gas molecules adsorbed in the IL. This could explain why the observed feature potential follows the same dependence, $V^{1/3} \approx D$ (Figure 1b).

In our classical MD simulations of the IL interface (Supporting Information), we have modeled $[C_4mpy][NTf_2]$ with solvated SO_2 gas molecules above a charged gold electrode, but resorted for simplicity to a nonpolarized surface. Figure 5a shows two simulated systems without (left) and with (right) SO_2 molecules. To calculate the distribution of SO_2 molecules away from the charged gold surface, we divided the IL into layers (bins) with a thickness of 1 Å. We chose a carbon atom of the pyrrolidine ring of the cation, a nitrogen atom of the anion, and a sulfur atom of SO_2, and we calculated the number of these atoms in each bin to obtain the distribution of corresponding ions and molecules. The averaging was done over the last 30 ns of simulations.

As shown in Figure 5c, the SO_2 population oscillates with a distance from the electrode, where the population in different peaks depends on the applied electric field. This SO_2 distribution is closely correlated with the uneven change of distributions of ions, as shown in Figure 5c and Figure S6. The first SO_2 peak (surface adsorption distance) appears at 4 Å above the surface, regardless of the electrode charging. Figure 5b illustrates the effect of electrode charging on the distribution of SO_2 in this first peak. The simulations show that its SO_2 population increases with the applied potential. At $-0.6e$, SO_2 adsorption is at the maximum, perhaps due to the polar nature of SO_2. The insets show that, beyond a certain potential, the number of SO_2 decreases, suggesting that SO_2 might be expelled from the surface by the ions that are more strongly attracted to the charged surface, despite their large sizes. If we assume that the gas molecules are expelled from the surface when their effective sizes, D, are smaller than the unoccupied space due to potential induced-ion rearrangements at the electrode interface, we can obtain a good agreement with the experimental observations, according to eq 3. The field-induced release of gas molecules from the interface causes rearrangement of the IL at the feature potential, giving the observed change of electrode capacitance due to the change of double layer thickness d.

DOI: 10.1021/acs.analchem.5b04677
Anal. Chem. 2016, 88, 1959−1964

CONCLUSIONS

In the presence of electric fields, the structures and properties of an IL at the electrode interface resemble crystalline solids that are significantly different from traditional electric double layers. In this work, we systematically characterized the differential capacitances of electrified IL−electrode interface in the presence of eight different gas molecules. The observed change of differential capacitance at the IL−electrode interface in the presence of gas molecules has a local maximum at a certain potential. This potential defined here as "feature potential" was found to be unique for each specific gas molecule, and the amplitude of the differential capacitance change at the feature potential is found to relate to the concentration of the gas molecules. The differential capacitance measurement of IL near an electrode at feature potential was utilized as a sensing interface for SO_2 detection. A reversible quantification of SO_2 at ppb levels with little interference signal from other interfering species was achieved. This IL−electrode interface-based capacitance sensor can offer high selectivity, long-term stability, good reversibility, and high sensitivity at low power and low cost and should allow new detection techniques and fabrication of new sensors through IL−electrode material engineering and interface design. In particular, the ability to tailor the ionic liquid chemistry coupled with electrochemistry at the electrode interface offers many opportunities in the advancement of electrochemical gas sensors for miniaturization toward integration into wearable sensors adapted to individual needs.

ASSOCIATED CONTENT

Supporting Information

The Supporting Information is available free of charge on the ACS Publications website at DOI: 10.1021/acs.analchem.5b04677.

Electrode and experimental setup; capacitance response with two different SO_2 gas feeding pathways; Bode plot of $[C_4mpy][NTf_2]$/Au system with different SO_2 concentrations; long-term stability measurements of SO_2 sensing; atomistic molecular dynamics (MD) simulations of the ionic liquid−Au electrode interface with solvated SO_2; distribution of cations and anions of $[C_4mpy][NTf_2]$ with the distance from the gold surface; measured kinetic diameter (KD) values of selected gas molecules (PDF)

AUTHOR INFORMATION

Corresponding Author

*E-mail: zeng@oakland.edu.

Notes

The authors declare no competing financial interest.

ACKNOWLEDGMENTS

Support from NIOSH grants (1R21OH009099-01A1 and 1R01OH009644-01A1) are greatly acknowledged. X.Z. thanks M. Sevilla for stimulating discussions and Norman Leo for his contributions in proofreading of this manuscript. The work of P.K. was supported by the NSF DMR Grant No. 1309765 and by the ACS PRF Grant No. 53062-ND6.

REFERENCES

(1) Rogers, R. D. *Nature* **2007**, *447*, 917−918.
(2) Armand, M.; Endres, F.; MacFarlane, D. R.; Ohno, H.; Scrosati, B. *Nat. Mater.* **2009**, *8*, 621−629.
(3) Cremer, T. In *Ionic Liquid Bulk and Interface Properties*; Springer International Publishing: 2013; pp 69−122.
(4) Kondrat, S.; Georgi, N.; Fedorov, M. V.; Kornyshev, A. A. *Phys. Chem. Chem. Phys.* **2011**, *13*, 11359−11366.
(5) Fedorov, M. V.; Kornyshev, A. A. *Chem. Rev.* **2014**, *114*, 2978−3036.
(6) Muller, E. A.; Strader, M. L.; Johns, J. E.; Yang, A.; Caplins, B. W.; Shearer, A. J.; Suich, D. E.; Harris, C. B. *J. Am. Chem. Soc.* **2013**, *135*, 10646−10653.
(7) McIntosh, E. M.; Ellis, J.; Jardine, A. P.; Licence, P.; Jones, R. G.; Allison, W. *Chemical Science* **2014**, *5*, 667−676.
(8) Atkin, R.; El Abedin, S. Z.; Hayes, R.; Gasparotto, L. H. S.; Borisenko, N.; Endres, F. *J. Phys. Chem. C* **2009**, *113*, 13266−13272.
(9) Endres, F.; Borisenko, N.; El Abedin, S. Z.; Hayes, R.; Atkin, R. *Faraday Discuss.* **2012**, *154*, 221−233.
(10) Vatamanu, J.; Borodin, O.; Smith, G. D. *J. Am. Chem. Soc.* **2010**, *132*, 14825−14833.
(11) Freyland, W. *Phys. Chem. Chem. Phys.* **2008**, *10*, 923−936.
(12) Kirchner, K.; Kirchner, T.; Ivaništšev, V.; Fedorov, M. V. *Electrochim. Acta* **2013**, *110*, 762−771.
(13) Baldelli, S. *Acc. Chem. Res.* **2008**, *41*, 421−431.
(14) Druschler, M.; Huber, B.; Passerini, S.; Roling, B. *J. Phys. Chem. C* **2010**, *114*, 3614−3617.
(15) Siinor, L.; Lust, K.; Lust, K. *Electrochem. Commun.* **2010**, *12*, 1058−1061.
(16) Artem, L. M.; Santos, D. M.; De Andrade, A. R.; Kokoh, K. B.; Ribeiro, J. *Sci. World J.* **2012**, *2012*, 502083.
(17) Ding, L. X.; Wang, A. L.; Li, G. R.; Liu, Z. Q.; Zhao, W. X.; Su, C. Y.; Tong, Y. X. *J. Am. Chem. Soc.* **2012**, *134*, 5730−5733.
(18) Welsch, F. G.; Stowe, K.; Maier, W. F. *ACS Comb. Sci.* **2011**, *13*, 518−529.
(19) Sattarahmady, N.; Heli, H.; Faramarzi, F. *Talanta* **2010**, *82*, 1126−1135.
(20) Ferrin, P.; Mavrikakis, M. *J. Am. Chem. Soc.* **2009**, *131*, 14381−14389.
(21) Feng, G.; Zhang, J. S.; Qiao, R. *J. Phys. Chem. C* **2009**, *113*, 4549−4559.
(22) Klähn, M.; Seduraman, A. *J. Phys. Chem. B* **2015**, *119*, 10066.
(23) Feng, G.; Jiang, X.; Qiao, R.; Kornyshev, A. A. *ACS Nano* **2014**, *8*, 11685−11694.
(24) Wang, Z.; Mu, X.; Guo, M.; Huang, Y.; Mason, A. J.; Zeng, X. *J. Electrochem. Soc.* **2013**, *160*, B83−B89.
(25) Pera-Titus, M. *Chem. Rev.* **2014**, *114*, 1413−1492.
(26) Tozawa, T.; Jones, J. T. A.; Swamy, S. I.; Jiang, S.; Adams, D. J.; Shakespeare, S.; Clowes, R.; Bradshaw, D.; Hasell, T.; Chong, S. Y.; Tang, C.; Thompson, S.; Parker, J.; Trewin, A.; Bacsa, J.; Slawin, A. M. Z.; Steiner, A.; Cooper, A. I. *Nat. Mater.* **2009**, *8*, 973−978.
(27) Wang, Z.; Lin, P.; Baker, G. A.; Stetter, J.; Zeng, X. *Anal. Chem.* **2011**, *83*, 7066−7073.
(28) Orazem, M. E.; Tribollet, B. *Electrochemical impedance spectroscopy*; Wiley InterScience: New York, 2008.
(29) Kornyshev, A. A. *J. Phys. Chem. B* **2007**, *111*, 5545−5557.
(30) Bates, E. D.; Mayton, R. D.; Ntai, I.; Davis, J. H. *J. Am. Chem. Soc.* **2002**, *124*, 926−927.
(31) Rodriguez, J. A.; Liu, G.; Jirsak, T.; Hrbek, J.; Chang, Z. P.; Dvorak, J.; Maiti, A. *J. Am. Chem. Soc.* **2002**, *124*, 5242−5250.
(32) Wang, Z.; Zeng, X. *J. Electrochem. Soc.* **2013**, *160*, H604−H611.
(33) Baldelli, S. *Acc. Chem. Res.* **2008**, *41*, 421−431.
(34) Weingartner, H.; Sasisanker, P.; Daguenet, C.; Dyson, P. J.; Krossing, I.; Slattery, J. M.; Schubert, T. *J. Phys. Chem. B* **2007**, *111*, 4775−4780.
(35) Snow, E. S.; Perkins, F. K.; Houser, E. J.; Badescu, S. C.; Reinecke, T. L. *Science* **2005**, *307*, 1942−1945.
(36) Loth, M. S.; Skinner, B.; Shklovskii, B. I. *Phys. Rev. E* **2010**, *82*, 056102.

DOI: 10.1021/acs.analchem.5b04677
Anal. Chem. 2016, 88, 1959−1964